ARTICLE

Everything in its right place: Controlling the local composition of hydrogels using microfluidic traps

Received 00th January 20xx,
Accepted 00th January 20xx

DOI: 10.1039/x0xx00000x

Michael Kessler,[a] Hervé Elettro,[b] Isabelle Heimgartner,[a] Soujanya Madasu,[a] Kenneth A. Brakke,[c] François Gallaire,[b] and Esther Amstad*[a]

Supplementary Information

This file includes:

Supplementary text
Figures S1 to S2
Legends for Movies S1 to S3

Other supplementary materials for this manuscript include the following:

Movies S1 to S3

Description of model for drops relaxing into spherical microfluidic traps

To describe the change in surface area of drops upon their trapping and the volume of the drop located in the trap, we model all parts of the drop with the same curvature. Note that the curvature is conserved in 3D, such that it is the product of the curvatures along two planes e.g. the xz-plane and the xy-plane. To describe the shape of the trapped drop, we integrate a curve revolving around the central z-axis of the trap along the z-direction. All the calculations for different trap geometries are given in Figure S1. We compare the resulting surface areas of our model to simulations, initially starting with a drop volume of 0.9 nL, as shown in Figure S1a. Our model is in excellent agreement with the Surface Evolver simulation data for traps with widths of 40 µm and 70 µm, as shown by orange filled squares and triangles in Figure S1a, respectively. We also calculate the surface area of drops trapped in traps with W = 100 µm and $p \leq 40$ µm. Also in this case, the model predictions agree well with the simulations, as shown by the blue filled circles in Figure S1a.

To extend our model we increase the trap depth p to 55 µm, even though we did not experimentally address these cases. In these cases $r < p$, such that the dome lies fully inside the trap; we color-coded this case purple. To describe the shape of drops in these traps, we add a cylinder with radius $W/2$ and height $(p - r)$ below the dome. A large volume fraction of the drops is located inside these deep traps such that the pancake in the channel starts to disappear; these cases are not captured properly by the model anymore. Although the error remains within 1% for p = 55 µm compared to simulations the surface area found with the model is underestimated and the results diverge, as shown in Figure S1a. To test the validity of our model for deep traps that immobilize larger drops, we increase the drop volume two-fold to 1.8 nL, while keeping the trap geometry unchanged. As long as the fraction of the drop located in the Hele-Shaw cell attains a pancake shape, our model shows excellent agreement with simulations, even if traps are as deep as 55 µm, as shown in Figure S1b. The error between the calculations and simulations for larger drops in deep traps remains below 0.3%.

We introduce a calculation tree that enables the quantification of the surface area change between the trapped and untrapped state of drops and the volume located in the trap. This information enables the prediction of the trapping force solely based on geometrical parameters h, p, W, R, as shown in Figure S1c. This part of the model is based on three different trapping regimes: Large and deep traps where $r < p$ and drops are described with a dome and a cylinder added below the dome, large traps where $r > p$ and the part of the drop contained in the trap forms a dome, and small traps where the part of the drop that relaxes into the trap forms a spherical cap. The three regimes are labeled as 1, 2, and 3, and color-coded in purple, blue, and orange, respectively in Figure S1c.

[a] *Soft Materials Laboratory, Institute of Materials, École Polytechnique Fédérale de Lausanne (EPFL), CH-1015 Lausanne, Switzerland.*
[b] *Laboratory of Fluid Mechanics and Instabilities, Institute of Mechanical Engineering, École Polytechnique Fédérale de Lausanne (EPFL), CH-1015 Lausanne, Switzerland.*
[c] *Mathematics Department, Susquehanna University, Selinsgrove, PA 17870, USA.*
Electronic Supplementary Information (ESI) available: [details of any supplementary information available should be included here]. See DOI: 10.1039/x0xx00000x

ARTICLE

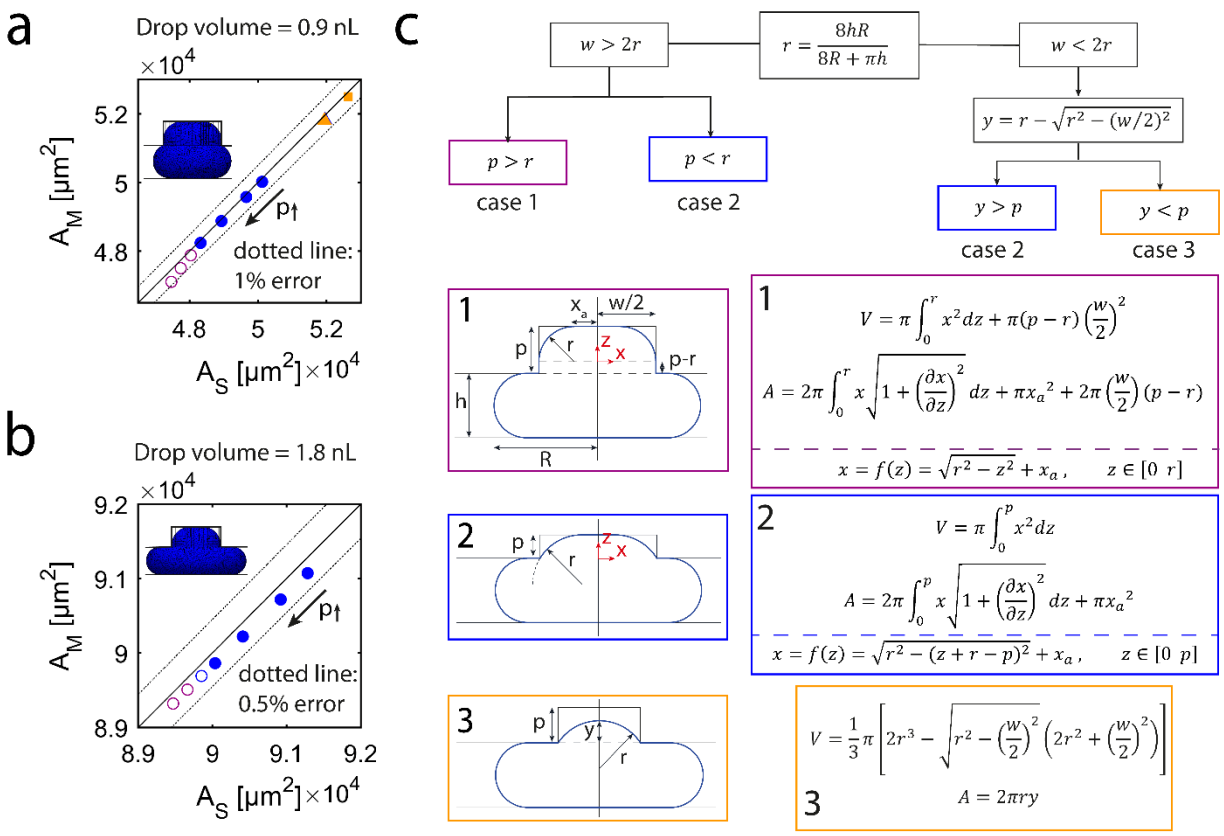

Figure S1: Model for quantifying the surface area change of drops between the trapped and untrapped state and the drop volume. a, b) Surface area obtained from the model A_M compared to the surface area obtained from Surface Evolver simulations A_S for a drop volume of (a) 0.9 nL and (b) 1.8 nL for spherical traps with W = 40 µm (squares), W = 70 µm (triangles), W = 100 µm (circles). Different data points with the same symbol indicate different trap depths p. The color code differentiates the different trapping regimes; dome with underlying cylinder (regime 1, purple), dome (regime 2, blue), and spherical cap (regime 3, orange). Empty symbols correspond to traps that were not experimentally addressed. The channel height was kept constant at h = 55 µm. Insets: Surface Evolver renderings of drops in traps with W = 100 µm and p = 40 µm. The straight line indicates $y = x$, and dotted lines indicate (a) 1% error and (b) 0.5% error. c) Three different trapping regimes. A calculation tree is presented to evaluate V and A. At first the radius of curvature r is calculated as a function of the pancake radius R and the channel height h. If $r > W/2$ a spherical cap deforms into the trap. The spherical cap can either freely deform into the trap, which leads to case 3, or is limited by the trap top, which leads to a flattening of the spherical cap and the formation of a dome, regime 2. If $r < W/2$ the drop forms a dome if $r > p$, case 2, or a dome with a cylinder below if $r < p$, case 1.

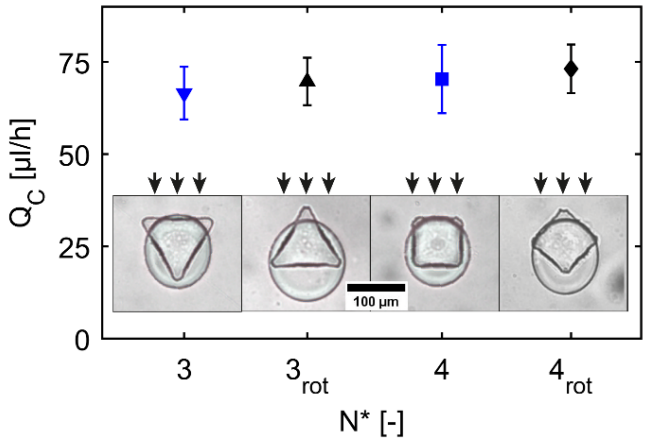

Figure S2: Influence of the orientation of triangular and square traps on Q_C. Q_C as a function of the number of corners of the polygonal trap N^* for two different orientations of traps. Insets: Micrographs of polygonal traps with different orientations relative to the flow of the continuous phase. Error bars represent the standard deviation and are calculated from at least 12 measurements.

References

1 C. Lv, 2017, 1–21.

2 Z. Nie, M. S. Seo, S. Xu, P. C. Lewis, M. Mok, E. Kumacheva, G. M. Whitesides, P. Garstecki and H. A. Stone, *Microfluid. Nanofluidics*, 2008, **5**, 585–594.

Movie S1 (separate file). Removal of drop from its trap as $\boldsymbol{Q > Q_C}$**.**

Movie S2 (separate file): Removal of drops from weak traps while flushing at a flow rate $Q_{C,S} < Q < Q_{C,H}$.

Movie S3 (separate file): Replacing the continuous oil phase with an aqueous phase containing precursors of the matrix.